Geomorphology 451 (2024) 109087

Contents lists available at ScienceDirect

Geomorphology

journal homepage: www.journals.elsevier.com/geomorphology

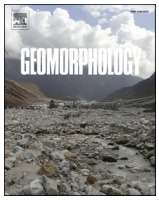

Morphodynamic and modeling insights from global sensitivity analysis of a barrier island evolution model

Steven W.H. Hoagland [a,c,*], Jennifer L. Irish [a,c], Robert Weiss [d,b,c]

[a] Dept. Civil and Environmental Engineering, Virginia Tech, 200 Patton Hall, 750 Drillfield Drive, Blacksburg, VA 24061, United States of America
[b] Dept. Geosciences, Virginia Tech, 4044 Derring Hall, 926 West Campus Drive, Blacksburg, VA 2061, United States of America
[c] Center for Coastal Studies, Virginia Tech, Blacksburg, VA 24061, United States of America
[d] Academy of Integrated Science, Virginia Tech, Blacksburg, VA 24061, United States of America

ARTICLE INFO

Keywords:
Barrier island
Modeling
Morphodynamics
Global sensitivity analysis

ABSTRACT

Recently developed models of coastal barrier morphodynamics include marsh and lagoon processes that have been shown to impact barrier island evolution. To gain additional insights into the simulated barrier-backbarrier system dynamics, this study explores the parameter space of a barrier evolution model using global sensitivity analysis. Influential parameters, their interactions with one another, and regions of sensitivity within the parameter space were identified using Sobol indices and factor mapping techniques for model results through the end of the century. The results of this study highlight an important relationship between initial and critical barrier island geometries and suggest that narrow and low-relief barriers are most vulnerable to be eroded away (width drowning) or overtaken by sea level rise (height drowning), respectively. Width drowning was also strongly associated with other model input parameters such as toe depth, sea level rise rate, and backbarrier critical bed shear stress, which suggests that sub-centennial drowning is dependent on a unique combination of input parameter values and may be averted (or delayed) with a single input parameter change. Barrier dynamics were significantly influenced by the backbarrier marsh platform, which was more impacted by sediment transport parameters such as critical bed shear stress and ocean sediment concentration than maximum annual overwash flux. This suggests that inorganic sediment deposition through tidal inlet dispersion is much more significant to the backbarrier marsh and lagoon system than overwash over sub-centennial timescales and can help to reduce the risk of width drowning.

1. Introduction

Barrier islands front an estimated 10% of the world's coastlines (Stutz and Pilkey, 2011) and provide a variety of socioeconomic benefits such as flood risk reduction (Grzegorzewski et al., 2011), recreation and tourism (Barbier et al., 2011). One of the most interesting features of barrier islands is that they are dynamic landforms; they change both shape and location in response to storm events and chronic changes in their environment such as sea level rise (SLR) and changes in sediment supply (e.g., Plant et al., 2017; Moore and Murray, 2018; McBride et al., 2022). Understanding the processes that drive the evolution of coastal barriers over decades or centuries and accurate prediction of future island states through modeling are two active and interdependent fields of research, both of which are necessary to effectively manage coastal resources.

In the 1980s and 90s, coastal evolution models of various type and formulation began to appear more frequently in the scientific literature (Hoagland et al., 2023). These early models ranged in complexity from one-line models of shoreline change (e.g., Pelnard-Considere, 1956; Hanson, 1989), to simplified 1D translation models (e.g., Bruun, 1962; Dean and Maurmeyer, 1983; Everts, 1985; Cowell et al., 1992), to two-dimensional and quasi-two-dimensional approaches (e.g., Bakker, 1968; Perlin and Dean, 1979; Larson et al., 1990; de Vriend et al., 1993; Niedoroda et al., 1995). Models also varied in their application, some applied to barrier island systems specifically (e.g., Dean and Maurmeyer, 1983; Cowell et al., 1992) and others to shorelines more generally (e.g., Bruun, 1962; Perlin and Dean, 1979; Hanson, 1989; de Vriend et al., 1993). In recent decades, new models have continued to be developed,

* Corresponding author at: Dept. Civil and Environmental Engineering, Virginia Tech, 200 Patton Hall, 750 Drillfield Drive, Blacksburg, VA 24061, United States of America.
E-mail address: shoagland@vt.edu (S.W.H. Hoagland).

https://doi.org/10.1016/j.geomorph.2024.109087
Received 5 September 2023; Received in revised form 27 January 2024; Accepted 30 January 2024
Available online 7 February 2024

many of which improve existing formulations and include processes that were not previously captured such as changes in alongshore sediment supply via inlet dynamics (e.g., Buijsman, 1997; Larson et al., 2002; Frey et al., 2012; Dean and Houston, 2016) overwash (e.g., Ashton and Murray, 2006; Storms et al., 2002; Stolper et al., 2005; Rosati et al., 2013; Lorenzo-Trueba and Ashton, 2014), dune growth and erosion (e.g., Rosati et al., 2010; Antolínez et al., 2019; Palalane and Larson, 2020; McCarroll et al., 2021; Reeves et al., 2021), and substrate consolidation by barrier migration (Rosati et al., 2006, 2010).

Sediment transport processes in the backbarrier marsh and lagoon system have also been included in barrier island models of the last two decades. Two notable models that include marsh-lagoon constituents are GEOMBEST+ (Walters et al., 2014) and the Lorenzo-Trueba and Mariotti (hereafter 'LTM17') model (Lorenzo-Trueba and Mariotti, 2017). These models attempt to capture the inherent complexity in the naturally-coupled barrier and backbarrier systems. The use of these models to explore the coupled system behavior across a variety of scenarios has yielded additional insights into long-term barrier dynamics. For example, Walters et al. (2014) found that narrow backbarrier marshes were sustained by barrier island overwash, which slowed the rate of barrier island transgression with sea level rise (SLR). Lorenzo-Trueba and Mariotti (2017) arrived at the same conclusion from their modeling study, finding that transgression rates were reduced by the presence of backbarrier marsh, which was impacted by overwash rates, inorganic sediment contributions, and lagoon geometry.

The numerical experiments conducted by Walters et al. (2014) and Lorenzo-Trueba and Mariotti (2017) were de facto sensitivity analyses in that they measured model output variability in response to changes in model input parameters. These studies also focused on long-term behavior over a 1000-year simulation time period. While the sensitivity analyses by Walters et al. (2014) and Lorenzo-Trueba and Mariotti (2017) yielded important insights, we hypothesize that a more thorough exploration of the parameter spaces over a shorter simulation time period may yield additional findings.

To gain additional insights into the simulated barrier-backbarrier system dynamics, our study simulates barrier evolution using the LTM17 model through year 2100, which may be in view at the end of some long-term planning horizons, and explores the model's input parameter space using global sensitivity analysis, which is a tool that can help modelers better understand the impact of their model's input parameters. Twenty of the LTM17 model's input parameters were evaluated in this study. These parameters are related to initial and equilibrium system geometries, external forcing conditions, and inorganic sediment transport, erosion, and deposition. More specifically, this study will focus on answering the following questions:

1. Which parameters significantly influence the model results?
2. Are there significant parameter interactions that influence the model results?
3. Are there regions of higher or lower sensitivity within the parameter space?

A variety of simulations and calculations were performed to address these questions. Input parameter sensitivities were characterized by estimating their contribution to the total model variance using the Sobol method (Sobol, 1993). Factor mapping was also used to explore the association of input parameter values with distinctive simulation categories (e.g., drowning) and regions within the parameter space. This analysis may be used to inform future modeling efforts in terms of understanding which parameters are most important to constrain, which parameters are relatively unimportant and can be fixed at a particular value, and which parameters should always be included as part of uncertainty analysis.

2. Lorenzo-Trueba and Mariotti (2017) model

The LTM17 model was created as a coupled reformulation of two previously published standalone models, namely the Lorenzo-Trueba and Ashton model (Lorenzo-Trueba and Ashton, 2014, hereafter 'LTA14') and the Mariotti and Carr model (Mariotti and Carr, 2014, hereafter 'MAC14'). The LTA14 model focuses on projecting changes in the barrier island itself, while the MAC14 model simulates changes in the backbarrier marsh and lagoon system. For a full description of the LTM17 model, the reader is referred to Lorenzo-Trueba and Mariotti (2017) and references therein.

The LTM17 model simulates long-term changes in both the barrier island and backbarrier (marsh and lagoon) subsystems. These subsystems are delineated in the model by six horizontal state variables: the toe position (X_T), shoreface position (X_S), backbarrier position (X_B), backbarrier marsh position (X_{M1}), interior marsh position (X_{M2}), and the mainland position (X_{M3}). Four vertical state variables, which include the barrier height (H_B), lagoon depth (D_F), and marsh depths (D_{M1}, D_{M2}), are also used to define the system geometry. Fig. 1 provides a graphical representation of the barrier subsystems and state variables. Together, simulated changes in these ten state variables are tracked over time through equilibrium-based sediment flux calculations, also shown in Fig. 1, including shoreface sediment flux (Q_{SF}), overwash flux (Q_{OW}), sediment flux between the shoreface and lagoon (I_{osl}), sediment flux between the lagoon and marshes (I_{bml} and I_{iml}), and biomass production within the marsh platforms (O_{bm} and O_{im}).

Shoreface sediment flux is calculated using the equilibrium profile assumption of Swart (1974), who found cross-shore sediment transport on the shoreface to be proportional to its deviation from an estimated equilibrium profile. Overwash flux is driven by the barrier's deficit volume, which is the volume of sediment required to extend the barrier's height (H_B) to a critical value (H_{cr}) such that overwash could no longer be deposited on the island, plus the volume of sediment required to extend the barrier's width (W_B) to a critical value (W_{cr}) such that overwash could no longer be deposited in the backbarrier system (Lorenzo-Trueba and Ashton, 2014). This idea of a barrier height or width that prevents overwash deposition originated as the 'Critical Length Concept' from Leatherman (1979). The volume deficit indicates the amount of sediment a barrier is able to accommodate before reaching its critical width and height; hence, the volume deficit is also commonly described as 'accommodation space' in the literature. Sediment is exchanged between the shoreface, lagoon, and marshes through tidal dispersion based on the relative concentration of sediments in each zone. Organic creation of marsh sediment and inorganic deposition of sediment in the marshes offset the loss of marsh elevation due to sea level rise and marsh erosion by backbarrier waves.

A number of 'result variables' may be calculated from the state variables shown in Fig. 1. For example, change in shoreline position (ΔX_S) is a result variable that may be calculated by subtracting the initial shoreline position (X_{S_0}) from the final shoreline position (X_{S_f}). Change in barrier width (ΔW_B) is another result variable that is calculated by subtracting the initial difference between the barrier and shoreline positions ($X_{B_0} - X_{S_0}$) and the final difference between the barrier and shoreline positions ($X_{B_f} - X_{S_f}$). The result variables considered in this study are presented in Table 1 with their state variable calculations and associated units. Note that many of the result variables involve calculations between the values at the beginning and end of the simulation to account for variations in the initial system geometry.

The LTM17 model has multiple strengths. One notable strength is its inclusion of marsh-lagoon processes, which relatively few barrier evolution models account for explicitly (Hoagland et al., 2023) and which have been shown to significantly impact barrier island evolution dynamics (e.g., Walters et al., 2014; Lorenzo-Trueba and Mariotti, 2017). Another strength of the model is its simplicity, from its transect-based setup to its straightforward state equations and Eulerian solution

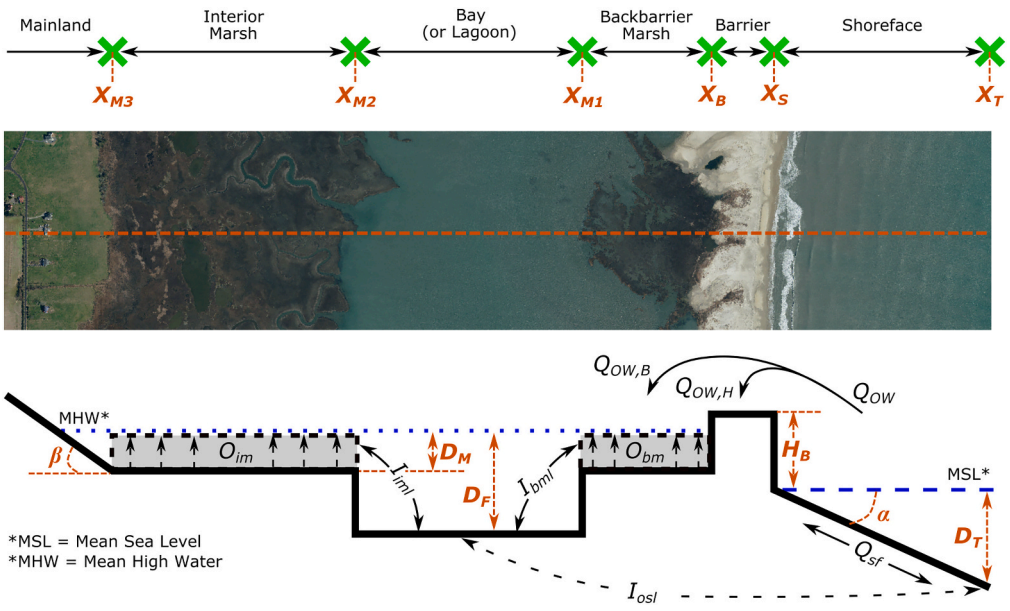

Fig. 1. Idealized barrier profile from LTM17 model.
Figure modified from Lorenzo-Trueba and Mariotti (2017). Aerial image of Assawoman Island section from (VGIN, 2021).

Table 1
LTM17 model result variables.

Result variable	Symbol	Calculation	Units
Change in shoreline position	ΔX_S	$(X_{S_f} - X_{S_0})$[a]	[m]
Change in barrier width	ΔW_B	$(X_{B_f} - X_{S_f}) - (X_{B_0} - X_{S_0})$	[m]
Change in barrier height	ΔH_B	$(H_{B_f} - H_{B_0})$	[m]
Change in backbarrier marsh width	ΔB_{M1}	$(X_{M1_f} - X_{B_f}) - (X_{M1_0} - X_{B_0})$	[m]
Change in lagoon width	ΔB_F	$(X_{M2_f} - X_{M1_f}) - (X_{M2_0} - X_{M1_0})$	[m]
Marsh depth	D_M	(D_{M1_f})	[m]
Lagoon depth	D_F	(D_{F_f})	[m]
Interior marsh width	B_{M2}	$(X_{M3_f} - X_{M2_f})$	[m]

[a] The f and 0 subscripts denote final and initial positions, respectively.

scheme. This simplicity leads to a relatively fast model runtime and gives the model a computational advantage over other, more complex models. This computational advantage allows modelers to evaluate parameter sensitivities toward a more robust understanding of the model and system dynamics, and to perform uncertainty analysis, which accounts for knowledge gaps and inherent parameter randomness in the final model projections.

However, these modeling advantages also come with certain assumptions and limitations which must be considered when interpreting the results. For example, model transects have a perfectly linear shoreface slope and rectangular representations of the subaerial island, marshes, and lagoon. This idealized transect geometry, combined with the equilibrium-based approach to sediment flux calculations, streamlines the model computations but can also lead to some oversimplifications. For example, the linearized shoreface slope is assumed to respond to deviations from the equilibrium value at a single rate, whereas in reality, we would expect the lower shoreface to respond more slowly than the upper shoreface (Stive and de Vriend, 1995; Ortiz and Ashton, 2016; Cowell and Kinsela, 2018). Another limitation stems from the absence of modeled dunes. The relationship between the water level and dune elevation is typically used to define the storm regime (e.g., Sallenger, 2000) which then has a direct impact on the barrier morphology (e.g., Long et al., 2014; Passeri et al., 2020). Additionally, washover is assumed to be deposited uniformly across the rectangular island and backbarrier marsh platform, whereas in reality, washover deposits become increasingly shallow toward the mainland (Carruthers et al., 2013).

2.1. Distinctive simulation categories

As the coupled barrier-backbarrier system evolves in the LTM17 model, there are four types of distinctive simulation categories in which the barrier system undergoes such a substantive change that the simulated processes that drive evolution of the system are no longer applicable. In such simulations the computations are either halted with results at the current timestep taken to be the final results, or significant geometry modifications are introduced. Simulations that do not fall into one of the distinctive categories described above are referred to as 'Normal' simulations, since they experience neither drowning nor lagoon infilling.

The first two distinctive simulation categories are those that result in barrier width drowning, referring to the condition in which the barrier island width reaches zero before the year 2100, and those that result in barrier height drowning for which the barrier height reaches zero before year 2100. The third type of distinctive simulation occurs when the marsh depth exceeds the maximum depth for marsh growth, which is referred to as marsh drowning. The fourth type of distinctive category is lagoon infilling, which occurs when the lagoon depth becomes equal to the marsh depth due to sediment deposition in the lagoon. In this type of simulation, the model's computation are not halted, but the marsh geometries are modified by setting the backbarrier marsh position (X_{M1}) equal to the barrier position (X_B) and the interior marsh position (X_{M2}) equal to the intersection position of interior marsh and the mainland (X_{M3}). This effectively eliminates the marsh widths when the lagoon fills and should be considered in the interpretation of the results.

2.2. Previous sensitivity studies

The findings of previous sensitivity studies are briefly highlighted below for comparison with the results of this study. At least four studies have been published that explore the sensitivity of the LTM17 model or its predecessor, the LTA14 model. The four studies were performed by Lorenzo-Trueba and Ashton (2014), Ashton and Lorenzo-Trueba (2015),

Lorenzo-Trueba and Mariotti (2017), and Ashton and Lorenzo-Trueba (2018).

In the first study of the LTA14 model, Lorenzo-Trueba and Ashton (2014) explored how interactions between key parameters such as maximum annual overwash flux ($Q_{OW,*}$), shoreface flux constant (K), SLR rate ($\dot{z}$), and mainland slope (β) influenced long-term behavior patterns. The authors found barrier systems to behave in one of four ways: 1) dynamic equilibrium, 2) periodic retreat, 3) barrier height drowning, and 4) barrier width drowning. Since their study was focused on long-term system behavior out to 1000 years, the authors evaluated how changes to input parameters affected the model's proclivity toward one of these four behaviors. Thus, parameters that did not impact the long-term oscillatory behavior pattern were considered insensitive.

In the second study, Ashton and Lorenzo-Trueba (2015) coupled the longshore model of Ashton and Murray (2006) with the LTA14 model to study the effects of sea level rise and longshore coupling over 400 years of barrier evolution. Using an initial shoreline disturbance of decreased width as the catalyst for system change, the authors found that increased sea level rise rates exacerbated the alongshore differences between adjacent island cross-sections. However, they also found that a stronger coupling between adjacent cross-sections could dampen these differences and had a significant impact on producing a smoothed, more uniform shoreline.

In the third study, Lorenzo-Trubea and Mariotti (2017) explored how larger initial lagoon widths (B_F), smaller ocean sediment concentrations (C_o), and smaller mainland slopes (β) affected system dynamics over 1000 years. They found that each of these parameters increased the accommodation space (either directly or indirectly) and lead to increased likelihood of width drowning.

In the fourth and most recent study, Ashton and Lorenzo-Trueba (2018) evaluated the impact of a changing mainland slope, and found that changes to the backbarrier slope directly impacted the accommodation space and associated behavior, similar to previous studies. Results from each of these studies are summarized in Table 2.

A common theme across the previous sensitivity analysis studies is a focus on millennial-scale, system-level behavior patterns. While these results shed light on system feedbacks, they do not explicitly consider system sensitivities over the short-term planning horizon, which may be given higher consideration in coastal management decisions. These studies also do not explore the full range of input parameter combinations and thus may not identify all relevant parameter interactions.

Table 2
Results from previous sensitivity studies.

Study[a]	Parameter[b]	Impact
LTA14	$\dot{z}(+)$	Increased width drowning; reduced by higher K and Q_{ow}.
LTA14	$K(+)$	Reduced width drowning; increased migration.
LTA14	$Q_{ow}(+)$	Reduced width drowning;[c] increased migration.
LTA14	$\beta(-)$	Increased width drowning and decreased migration.
LTA14[d]	$W_0(+/-)$	Insignificant impact on long-term behavior.
LTA14[d]	$V_{D,MAX}(+)$	Increased dynamic equilibrium; decreased periodic retreat.
LTA14[d]	$D_T(+)$	Requires increased Q_{ow} and K to maintain equilibrium.
LTA14[d]	$W_{cr}(-)$	Increased width drowning.
ALT15	$\dot{z}(+)$	Increased and sustained change between cross-sections.
ALT15	$d_{sh}(-)$[e]	Increased and sustained change between cross-sections.
LTM17	$B_{F,0}(+)$	Increased marsh erosion and width drowning.
LTM17	$C_0(-)$	Increased width drowning; decreased migration.
LTM17	$\beta(-)$	Increased lagoon depth and width drowning.
ALT18	$d\beta/dx(+)$	Decreased accommodation space; increased migration.
ALT18	$d\beta/dx(-)$	Increased accommodation space and width drowning.

[a] LTA14: Lorenzo-Trueba and Ashton (2014); ALT15: Ashton and Lorenzo-Trueba (2015); LTM17: Lorenzo-Trueba and Mariotti (2017); ALT18: Ashton and Lorenzo-Trueba (2018).

[b] Signs following the parameter should be read as an increase or decrease in that parameter leading to the associated impact. E.g., '$\dot{z}(+)$' should be read, 'An increase in $\dot{z}$ leads to… [associated impact].'

[c] Exception: high Q_{ow} can diminish shoreface sediment and lead to drowning.

[d] Published in Lorenzo-Trueba and Ashton (2014) supporting information.

[e] Shoreline diffusivity constant (proxy for alongshore coupling).

3. Methodology

For this study, the Sobol method, developed in 1993 by Russian mathematician Ilya M. Sobol (Sobol, 1993), was selected due to its widely recognized robustness as a global sensitivity analysis method and its ability to identify parameter interactions. As of 2016, this method was considered to be one of the "most sophisticated [sensitivity analysis] approach[es] developed to-date" (Razavi and Gupta, 2016).

3.1. Sobol method overview

The Sobol method involves calculating sensitivity indices for each input parameter that quantifies the percentage of model variance accounted for by that input parameter individually and interactively. Higher index values are associated with more sensitive parameters. In this study, three types of Sobol indices are calculated: (1) first order indices, (2) k-th-order indices, where k is the total number of input parameters being evaluated, and (3) interaction indices.

The first order index for a given input parameter, also commonly referred to as a parameter's 'main effect,' is defined as the variance of the conditional mean associated with fixing said parameter at a given value, divided by the total variance. Mathematically, the first order index (S_i) is as follows:

$$S_i = \frac{V(E(Y|X_i))}{V(Y)} \tag{1}$$

where $V(E(Y|X_i))$ is the variance of the expected value, or mean, of the model output (assuming sufficiently many model simulations for stability) given that parameter X_i is fixed at a randomly sampled value in its range, and $V(Y)$ is the total model variance. This calculation produces S_i values between 0 and 1, with higher S_i values indicating greater sensitivity. Because the index calculation involves expected values (means) and variances, the index values will become increasingly stable as more simulations are performed. Conversely, too few simulations increase the likelihood of numerical error in the results.

In many models, input variables often interact with one another so as to amplify or dampen their impact on the results. The Sobol method's k-th order index, more commonly called the 'total effect,' captures a parameter's main effect and all other higher-order or interactive effects. Mathematically, the calculation is represented by:

$$S_{T_i} = 1 - \frac{V(E(Y|X_{\sim i}))}{V(Y)} \tag{2}$$

where $E(Y|X_{\sim i})$ is the conditional mean of the model output associated with fixing the value of all parameters *except* for X_i.

The k-th order Sobol index provides a couple of important insights. First, if the k-th order index is zero or near zero, then it may be concluded that the factor does not significantly contribute to the total model variance and can therefore be fixed at any value in its range. Second, by subtracting the first order index from the k-th order index, the impact of the parameters' interactions is isolated - this metric is referred to herein as an 'interaction index.' Therefore, if there is a significant difference between the first and k-th order indices for a given parameter (i.e., if its interaction index is large), that particular parameter, it may be concluded, significantly contributes to the results through one or more interactions.

3.2. Model parameterization

Twenty input parameters were selected for evaluation in this sensitivity study. Since the Sobol Method requires numerous model simulations and randomly sampled input parameter values, each input

parameter was assigned a value range that defined the upper and lower limits of the sampling range. Parameter ranges were selected for this study based on typical ranges or values that have been justified and used in previous studies including Lorenzo-Trueba and Ashton (2014), Mariotti and Carr (2014), Lorenzo-Trueba and Mariotti (2017), and Miselis and Lorenzo-Trueba (2017). A comparison of this study's parameter ranges to those of previous studies is presented in Table S1.1 of the Supplementary material. The 20 input parameters are presented in Table 3 with their value range and units. Each parameter was also broadly categorized as influencing the system geometry, forcing conditions, or sediment transport calculations. Initial geometries of the system were also randomized for this sensitivity study to determine the influence of a system's current state on its long-term evolution; some of these initial geometries were also later constrained to evaluate their impact (see Section 3.3). The sensitivity of the 20 input parameters was evaluated for each result variable in Table 1.

3.3. Simulation sets

Three sets of simulations were performed to answer the proposed research questions. For all of the simulations described below, randomized input parameter values were sampled from a uniform distribution across their value range.

To gain a preliminary understanding of model behavior, we ran 50,000 simulations with fully randomized input parameter values and used factor mapping to associate the parameter values with the distinctive simulation categories described in Section 2.1. These simulations required approximately 3.59 CPU-hours and are hereafter referred to as Simulation Set A. Since initial barrier geometries and critical bed shear stress were found to significantly impact the model results toward drowning and lagoon filling (see Section 4.1), the geometry parameters were fixed at their average range values and the shear stress parameter was constrained (maximum 0.2 Pa) for the other simulations.

To calculate numerically stable first order and *k*-th order Sobol indices for input parameters (Table 3) and result variables (Table 1), 250,000 model simulations were run per input parameter. A total of 5 million simulations were run for conditional variance calculations which required 346 CPU-hours. These simulations are hereafter referred to as Simulation Set B. Input parameter values were randomly generated and index values were calculated following the matrix resampling procedure described in Saltelli et al. (2008).

To explore specific parameter interactions and regions of sensitivity within the parameter space, we again ran 50,000 simulations with fully randomized input parameters. This set of simulations required approximately 3.59 CPU-hours and is hereafter referred to as Simulation Set C.

Table 3
LTM17 model input parameters.

Symbol	Input parameter	Value range	Units	Category[a]
β	Mainland slope	0.0001–0.005	[m/m]	Geometry
D_T	Toe depth	5–15	[m]	Geometry
W_{cr}	Critical width	100–600	[m]	Geometry
H_{cr}	Critical height	0.5–4	[m]	Geometry
W_0	Initial width	100–1,000	[m]	Geometry
H_0	Initial height	0.5–4	[m]	Geometry
α_e	Equilibrium shoreface slope	0.005–0.025	[m/m]	Geometry
$B_{M1,cr}$	Critical backbarrier marsh width	50–500	[m]	Geometry
$B_{M1,0}$	Initial backbarrier marsh width	50–1,000	[m]	Geometry
$B_{F,0}$	Initial lagoon width	1,000–10,000	[m]	Geometry
$D_{F,0}$	Initial lagoon depth	1–3	[m]	Geometry
$Q_{OW,*}$	Max. annual overwash flux	1–100	[m^3/m/yr]	Forcing
$\dot{z}$	Sea level rise rate	3–20	[mm/yr]	Forcing
K	Shoreface flux const.	100–10,000	[m^3/m/yr]	Forcing
U_{ref}	Reference Wind speed	5–10	[m/s]	Forcing
r	Tidal range	0.7–2.8	[m]	Forcing
ω_s	Sediment settling velocity	0.05–0.5	[mm/s]	Sediment
τ_{cr}	Critical bed shear stress	0.05–0.4	[Pa]	Sediment
C_o	Ocean sediment conc.	30–200	[mg/l]	Sediment
B_P	Peak biomass production	1.5–3.5	[kg/m^2]	Sediment

[a] The categories indicate the general nature of the input parameter; some alter the system geometry others the forcing conditions, and some the sediment transport.

4. Results

4.1. Preliminary results

Select results from Simulation Set A are presented in the boxplots in Fig. 2 (see Figs. S2.1 through S2.4 in the Supplementary material for all results). Comparing these boxplots to one another allows us to see whether an input parameter significantly influences the model toward a drowning and/or filling scenario, which should be taken into consideration in the interpretation of results. Statistically significant differences between each category's median value and the ALL category median value were identified by non-overlapping 95% confidence intervals and are indicated by gray-colored boxplots. Confidence intervals are provided in the Supplementary material in Tables S2.1-S2.4 and S4.1-S4.3.

The initial and critical barrier geometry parameters (W_0, H_0, W_{cr}, H_{cr}) were found to be most influential on the barrier results. Low values of initial barrier width were strongly associated with width drowning simulations (Fig. 2a) while low values of initial barrier height were strongly associated with height drowning simulations (Fig. 2b). Significant interaction indices and heatmap plots of the preliminary results confirm that a significant interaction is present between the initial geometries and critical geometries (see Fig. S3.1 in the Supplementary material). The barrier geometry tends to increase when critical geometry is greater than initial geometry, and the barrier geometry decreases when critical geometry is less than initial geometry.

Preliminary results also show that critical bed shear stress (τ_{cr}) significantly influences the simulation toward lagoon filling and/or drowning, as noted by the statistically significant difference between the ALL and NRM medians in Fig. 2c. Since the WD and HD boxplots greatly overlap NRM but the FIL boxplot does not, it may be concluded that high τ_{cr} values drive the model toward lagoon filling.

In addition to showing general tendencies or associations, the boxplots in Fig. 2 also show parameter thresholds. For example, the results suggest that barrier drowning does not typically occur when initial barrier width is above 400 m. Similarly, height drowning does not occur when initial barrier heights are above 3 m, and lagoon filling does not occur when the critical bed shear stress is below 0.2 Pa.

4.2. Influential parameters

From Simulation Set B, the first and *k*-th order Sobol indices were calculated for each combination of input parameter (Table 3) and result variable (Table 1). These results are presented graphically in Fig. 3.

From Fig. 3a, it may be observed that most input parameters tended to impact a subset of result variables, the exception being SLR rate ($\dot{z}$), which influenced a majority of the results. However, in Fig. 3b, parameters were more influential over many different result variables. In addition to SLR rate ($\dot{z}$), reference wind speed (U_{ref}), tidal range (r), critical bed shear stress (τ_{cr}), and the ocean sediment concentration (C_o) all show at least moderate influence for most result variables. Other parameters such as the shoreface equilibrium slope (α_e), critical backbarrier marsh width ($B_{M1,cr}$), shoreface flux constant (K), sediment settling velocity (ω_s), and peak biomass production (B_P) had zero (or near-zero) Sobol indices for many of the results, suggesting these parameters were relatively non-influential.

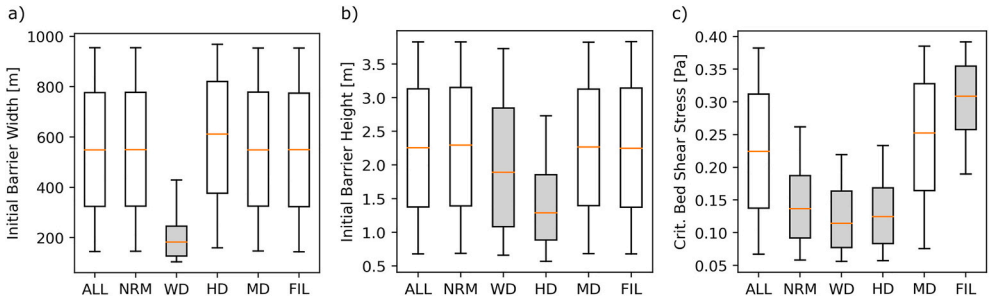

Fig. 2. Distinctive simulation category boxplots for Simulation Set A by input parameter for (a) initial barrier width, (b) initial barrier height, and (c) critical bed shear stress. Input parameters are shown on the y-axes. Each boxplot represents the 5th, 25th, 50th, 75th, and 95th percentiles, from bottom to top. Distinctive simulation categories are represented on the x-axes: ALL = all simulations/scenarios; NRM = normal (no drowning/filling); WD = width drowning; HD = height drowning; MD = marsh drowning; FIL = lagoon filling.

Similar to the preliminary results, critical barrier geometries (W_{cr} and H_{cr}) were highly significant for the barrier results. Changes in barrier width and shoreline position were also influenced by the barrier toe depth (D_T). Forcing conditions such as maximum annual overwash flux ($Q_{OW,*}$) and SLR rate ($\dot{z}$) influenced the barrier results individually, while other forcing parameters such as wind speed (U_{ref}) and tidal range (r), and sediment transport parameters such as critical bed shear stress (τ_{cr}) and ocean sediment concentration (C_o), showed low to moderate influence on the barrier results through interactions. The backbarrier results were also consistently influenced by the same forcing conditions and sediment transport parameters. Backbarrier geometry parameters tended to influence one or two related result variables. Mainland slope (β) influenced interior marsh and lagoon widths; the initial backbarrier marsh width ($B_{M1,0}$) influenced the backbarrier marsh and lagoon widths; and the lagoon results were influenced by the initial lagoon width ($B_{F,0}$) and initial lagoon depth ($D_{F,0}$).

The influence of parameters may also be seen in their association with distinctive simulation categories from Section 2.1. Boxplots were generated for each input parameter from the 50,000 fully randomized simulations in Simulation Set C. Select results are presented in Fig. 4 (see Fig. S4.1 in the Supplementary material for all results). Of the 50,000 total simulations, 0.3% resulted in width drowning, 3.2% resulted in marsh drowning, and 4.0% resulted in lagoon filling. There were no height drowning simulations in Simulation Set C. These drowning scenario numbers exclude cases where lagoon filling lead to drowning. Of the lagoon filling scenarios, 6.0% ended in width drowning and 66% ended in marsh drowning. Thus, only 28.0% of lagoon filling scenarios did not lead to drowning of the marsh or barrier island.

From Fig. 4, width drowning simulations are associated with low values of toe depth, critical bed shear stress, and ocean sediment concentration, and high values of critical barrier width, SLR rate, and wind speed. Marsh drowning simulations correspond to high SLR rate and low ocean sediment concentration, and lagoon filling is associated with low wind speed, high critical bed shear stress, and high ocean sediment concentration.

4.3. Interactions and sensitive regions

Interaction indices were calculated for each input parameter and result variable combination from Simulation Set B. These indices, presented in the heatmap in Fig. 5, show that the most interactive parameters are wind speed (U_{ref}), tidal range (r), critical bed shear stress (τ_{cr}), and ocean sediment concentration (C_o), which have very high index values for marsh depth, and relatively high indices across most other result variables. SLR rate ($\dot{z}$) also has moderately high interaction indices across the result variables. Maximum annual overwash flux ($Q_{OW,*}$) is highly interactive for the barrier results, but is not interactive with the backbarrier. Critical barrier geometries (W_{cr} and H_{cr}) are primarily interactive with the barrier system, with critical barrier width also impacting the backbarrier marsh width. Initial backbarrier marsh width ($B_{M1,0}$) interactions impact both the marsh width and transgression rates, and initial lagoon width ($B_{F,0}$) interactions impact marsh depth and to a lesser extent, barrier width and transgression.

While the relative interactivity of the input parameters and result variables may be known from the interaction indices, it is not always apparent which parameters interact and to what effect. From Fig. 5, the most interactive parameters for each result variable were identified and used to generate heatmaps using factor mapping from Simulation Set C in Figs. 6 and 7. In Fig. 6, it should be noted that for each of the results (e.g., barrier height: panes a-c), each pane shows one of the three combinations; thus, all three panes combined give a glimpse of the 3-dimensional parameter space.

Interactions for the barrier results primarily involve critical/initial geometry parameters and forcing conditions. Larger critical geometries are associated with greater barrier heights and widths and greater changes in shoreline position (Fig. 6a, b, d, e, g, h). However, this relationship is offset by lower values of overwash flux, SLR rate, and initial marsh width, and by greater values of toe depth. Overwash flux also interacts with SLR rate, initial marsh width, and toe depth to influence the barrier height, width, and transgression results, respectively.

In the backbarrier, initial marsh width controls the change in marsh width results for large critical barrier widths; however, low critical barrier widths significantly reduce the changes in marsh width (Fig. 7a). Interior marsh widths are significantly increased by low mainland slopes and high SLR rates (Fig. 7b). Larger values of critical bed shear stress tend to increase marsh depth and lagoon width but only for low values of wind speed (Fig. 7c, d). Higher critical bed shear stress is also associated with more significant reductions in lagoon depth, particularly for low initial lagoon widths (Fig. 7e).

Figs. 6 and 7 also show regions of sensitivity or nonlinearities within the parameter space. For greater critical barrier heights and widths, a significant nonlinearity is observed in the overwash flux parameter between 5 and 10 $m^3/m/yr$ for all of the barrier results. Nonlinearities are also observed for barrier width and transgression results where the critical barrier width nears the initial width. For the backbarrier results, significant nonlinearities are observed for the interior marsh width when mainland slope is lower than 0.001 m/m, and for marsh depth when critical shear stress exceeds 0.15 Pa for lower wind speeds.

5. Discussion

Initial and critical island geometry were found to significantly influence the barrier results, both individually and interactively, over the 100-year simulation period. This is because the model was formulated using the critical length concept of Leatherman (1979), which acts as a pseudo-equilibrium formulation that determines where and when overwash flux occurs. The critical length concept was based on Leatherman's observation of a barrier island that narrowed to an observed

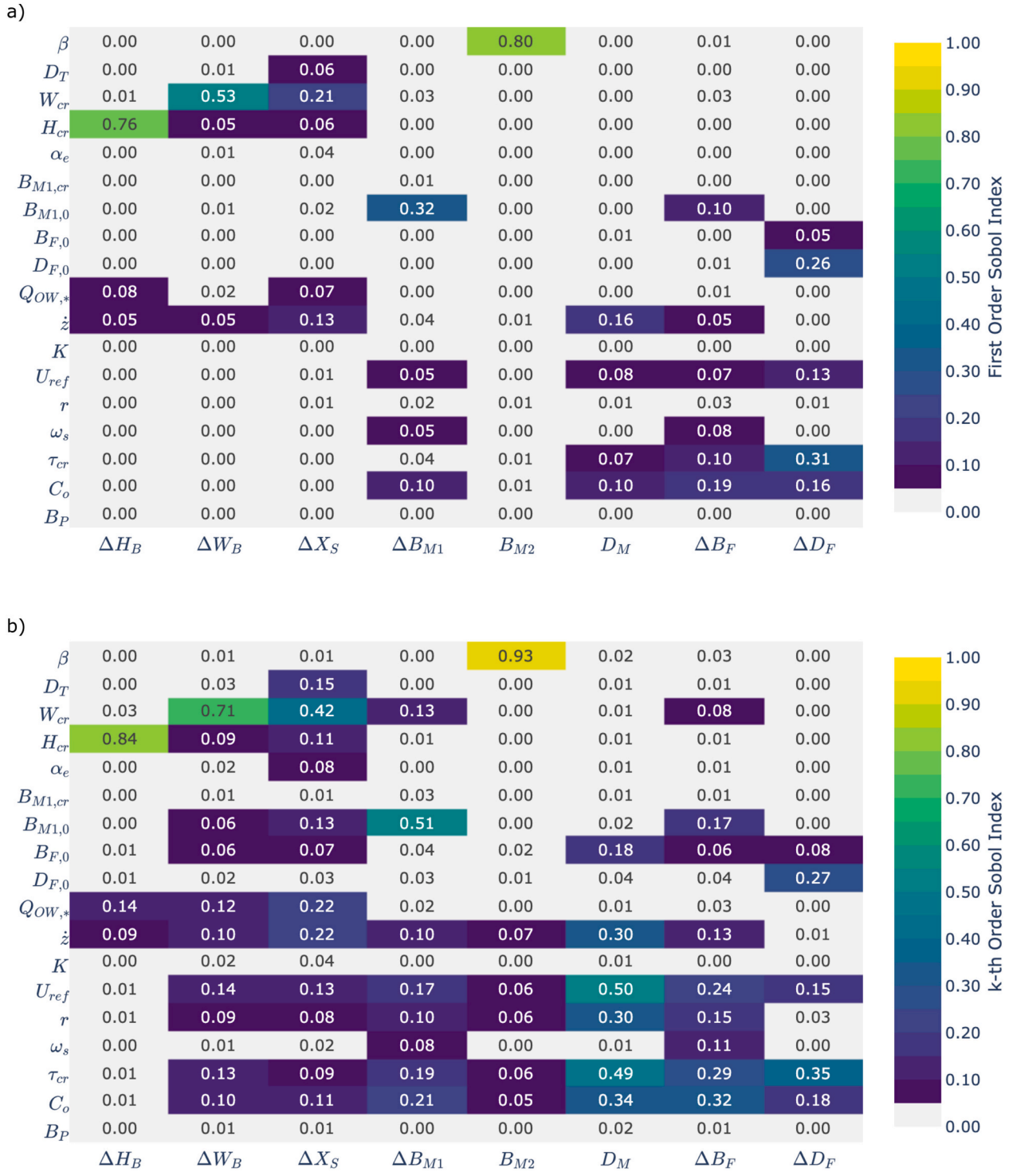

Fig. 3. Heatmaps of (a) first order indices and (b) *k*-th order indices from Simulation Set B. Result variables are shown on the x-axes according to their symbols, and input parameters are shown on the y-axes according to their symbols.

threshold, or critical width, before experiencing higher rates of transgression, where the overwashed sediment could reach the backbarrier to offset shoreline erosion (Leatherman, 1979). This phenomenon was also noted in the subsequent work of Everts (1987), who found barrier retreat rates were notably less than preceding rates due to the islands' narrowing states. Robbins et al. (2022) have shed additional light on this phenomenon in a more recent study of a U.S. East Coast barrier island chain. Therein, a proposed conceptual model shows eroded sediment from narrowing barriers helps to sustain the width of downdrift neighboring islands, which maintains their low retreat rates. The model results presented herein clearly demonstrate this well-documented behavior, where the change in shoreline position is greatly increased when the initial barrier width is less than or equal to the critical barrier width (Supplemental material Fig. S.3.1c, f), or when the critical barrier width is comparatively large (Fig. 6g, h). The interaction plots indicate that critical geometries act as an equilibrium anchoring point to which the system naturally gravitates.

Initial island geometry was also found to have significantly

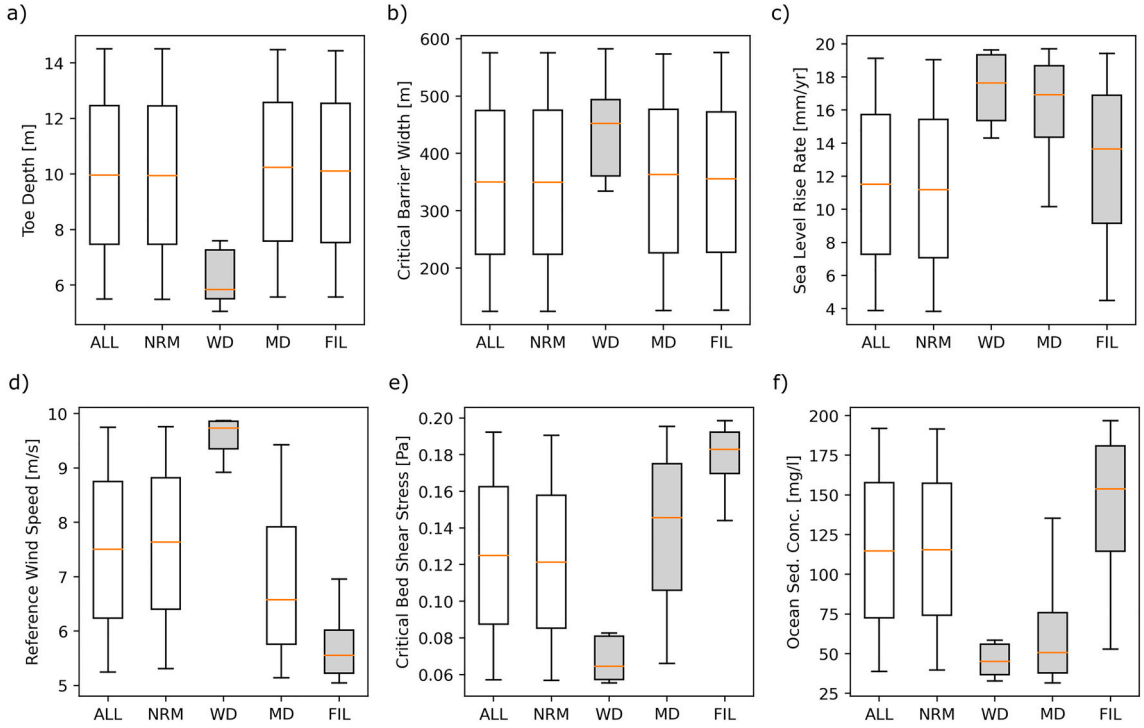

Fig. 4. Distinctive simulation category boxplots for Simulation Set C by input parameter for (a) toe depth, (b) critical barrier width, (c) sea level rise rate, (d) reference wind speed, (e) critical bed shear stress, and (f) ocean sediment concentration. Input parameters are shown on the y-axes. Each boxplot represents the 5th, 25th, 50th, 75th, and 95th percentiles, from bottom to top. Distinctive simulation categories are represented on the x-axes: ALL = all simulations/scenarios; NRM = normal (no drowning/filling); WD = width drowning; MD = marsh drowning; FIL = lagoon filling. There were no height drowning simulations in this simulation set.

Fig. 5. Heatmap of interaction indices ($S_{Ti} - S_i$) from Simulation Set B.

influenced whether or not barriers experienced sub-centennial width drowning or height drowning. From Simulation Set A, barriers that were more than 450 m wide (the 39th percentile of the barrier width range) rarely experienced width drowning and barriers greater than 3 m high (the 71st percentile of the barrier height range) rarely experienced height drowning during the multi-decadal simulation period (Fig. 2a, b). This expands on and confirms our understanding gained from previous studies, which focused more on the behavioral tendencies of barrier islands toward drowning, periodic retreat, or dynamic equilibrium over centuries. For example, Lorenzo-Trubea and Ashton (2014) found that long-term behavior was not significantly influenced by initial geometry parameters as the initial system trajectories would reverse course

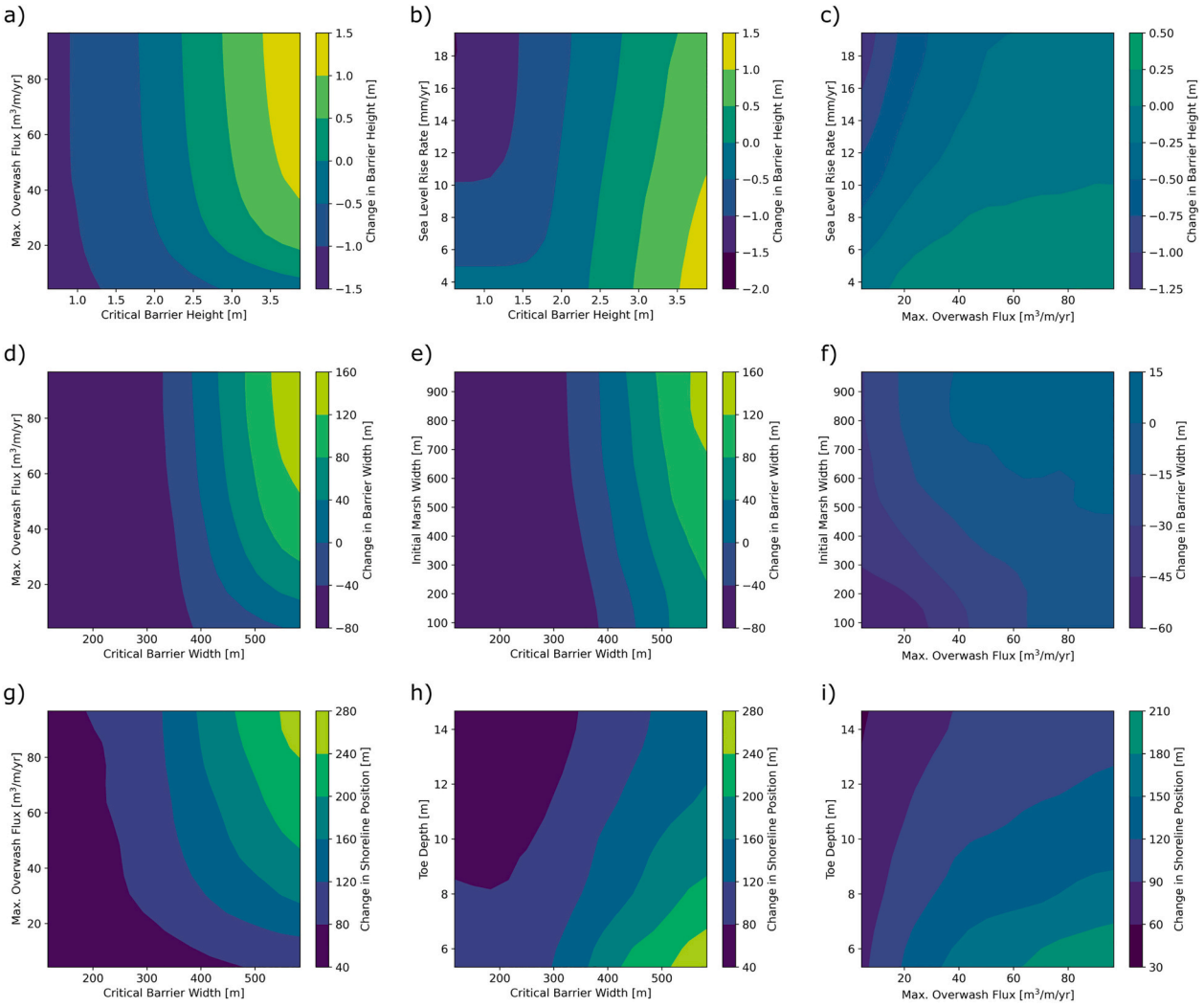

Fig. 6. Heatmaps of parameter interactions for barrier results (Simulation Set C).

toward dynamic equilibrium values over time; however, they did find that width drowning was associated with decreases in critical barrier width. This is likely a result of the phenomenon previously discussed, that a low critical width drives the system toward a sustained low-width equilibrium state that is more likely to drown as ocean-side erosion outpaces backbarrier expansion toward the mainland (e.g., Lorenzo-Trueba and Ashton, 2014; Ashton and Lorenzo-Trueba, 2015).

The results from this study suggest that moving boundaries (i.e., changes in height, width, and shoreline position) of barrier islands through the end of the 21st century will be most significantly influenced by the relationship between the initial and critical geometries and that narrow and low-relief barriers are most vulnerable to width drowning and height drowning, respectively. While barrier drowning is certainly significant, the question remains whether the boundary changes in non-drowning simulations are of any consequence. Wolinsky and Murray (2009) concluded that even though initial geometries could influence short term shoreline changes, long-term trends would be independent of such influences and would be controlled primarily by the substrate slope, which was demonstrated in subsequent numerical experiments conducted by Moore et al. (2010) and Murray and Moore (2018). For barriers that transgress in a state of periodic retreat, short term changes in barrier geometry could be irrelevant, since the barrier system might shift back toward its dynamic equilibrium state and prograde during the next cycle (Lorenzo-Trueba and Ashton, 2014). However, a more recent modeling study by Ciarletta et al. (2019) showed that it is possible for dynamic forcing conditions to interrupt the stability of these cycles. In this study, the authors showed that sudden changes or 'pulses' in SLR could modify depositional patterns and increase a barrier's potential for drowning (Ciarletta et al., 2019). Therefore, short term boundary changes from initial and critical geometries may impact the sustainability of barriers, even those which are in a presently stable form of retreat.

Width drowning simulations showed a remarkable association not only with critical and initial widths, but also with multiple other parameters including low toe depth ($\leq$8 m), low initial marsh width ($\leq$350 m), high initial lagoon width ($\geq$6500 m), high rates of SLR rate ($\geq$15 mm/yr), high reference wind speeds ($\geq$9 m/s), low critical bed shear stress ($\leq$0.08 Pa), and low ocean sediment concentration ($\leq$60 mg/l) (Fig. 4; Supplemental material Fig. S4.1). The significance of most of these parameters regarding width drowning confirms the findings of previous studies summarized in Table 2, including Lorenzo-Trueba and Ashton (2014), Ashton and Lorenzo-Trueba (2015), Lorenzo-Trueba and Mariotti (2017), and Ashton and Lorenzo-Trueba (2018). However, to the authors' knowledge, these results are the first to show that modeled short-term width drowning is dependent on the unique combination of these parameters. Taken together, the statistically significant parameter associations suggest that all are required for width drowning to occur within the multi-decadal simulation time period. It also indicates that if one or more of these parameters falls outside of the ranges described above, through either natural or anthropogenic changes, then width

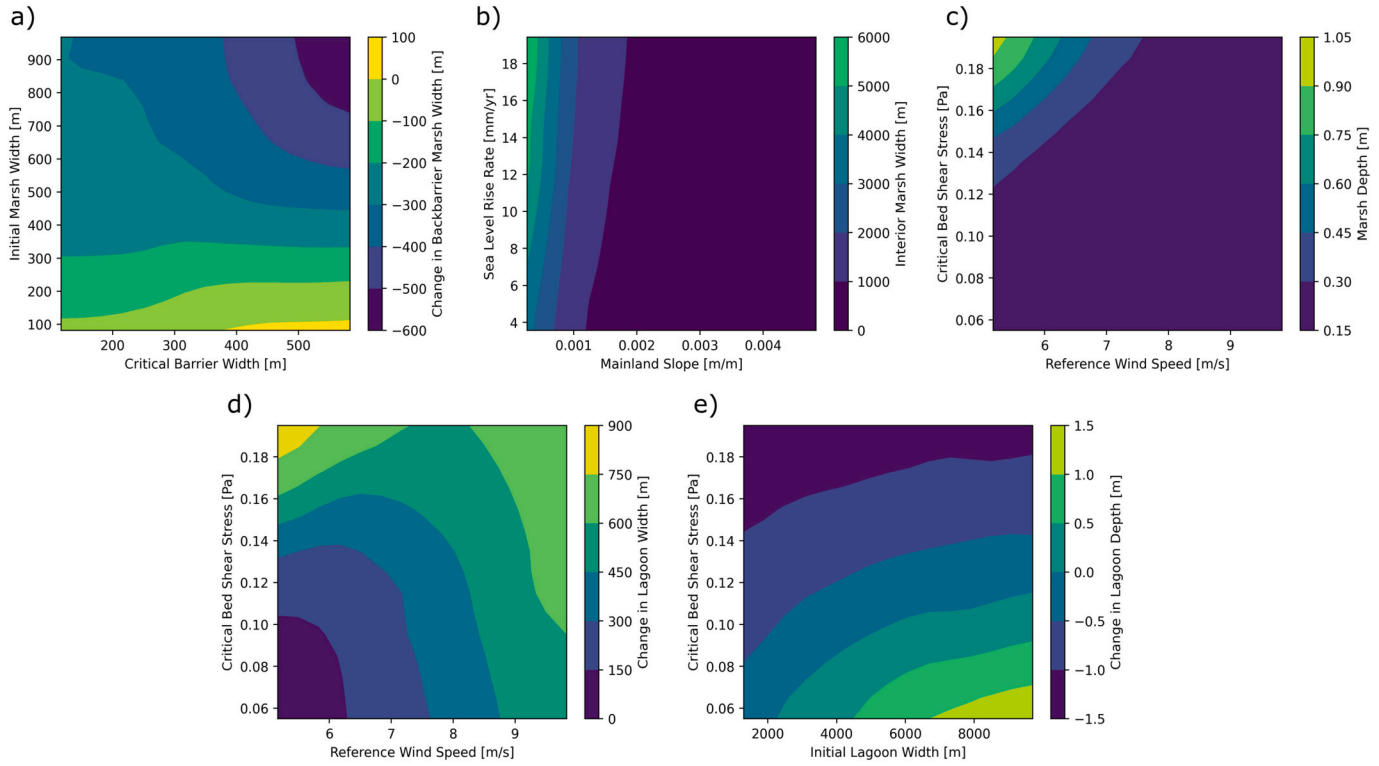

Fig. 7. Heatmaps of parameter interactions for backbarrier results (Simulation Set C).

drowning can be avoided in the short term or at least delayed. Such results may be used to inform localized alternatives analysis of nature-based solutions (Bridges et al., 2015) or other viable coastal restoration practices.

Barrier width and shoreline position were also influenced by the equilibrium shoreface slope and the shoreface toe depth, the latter being more significant (Fig. 3). Toe depth was found to influence transgression through interactions with critical barrier width and overwash flux (Figs. 5, 6h, i), and lower toe depth values were associated with width drowning (Fig. 4a). These influences are a result of conservation of mass from the nearshore-shoreface boundary to the barrier-backbarrier marsh boundary. In the model formulation, overwash volume that is deposited on or behind the barrier is eroded from the shoreface and ocean side of the island (Lorenzo-Trueba and Mariotti, 2017). Thus, all else being equal, islands with smaller toe depths have less available sediment for transport by overwash than islands with larger toe depths, meaning that islands must migrate larger distances to balance the eroded and deposited sediment volumes. This finding is consistent with other published studies that found a relationship between decreased sediment supply and increased island transgression (e.g., Moore et al., 2007, 2010; Brenner et al., 2015).

Furthermore, because toe depth is defined as the depth of the toe or seaward extent of the active shoreface profile, it can also be connected with the equilibrium profile concept of closure depth, which marks the location at which temporal profile adjustments due to changes in wave climate becomes negligible, effectively separating the active profile from the inactive profile (Hallermeier, 1977, 1980). While this depth threshold of shoreface activity is well-recognized and implemented in various models (e.g., Bruun, 1962; Cowell et al., 1995; Lorenzo-Trueba and Ashton, 2014), it has been shown that the time frame over which the simulation or study is conducted will impact the threshold, with longer time frames being associated with greater closure depths (Nicholls et al., 1998; Cowell et al., 2003). It has also been shown that modifying toe depth based on accelerations in SLR rate can also have a significant impact on transgression rates (Cowell and Kinsela, 2018).

One surprising result was the relative insignificance of the mainland slope parameter across the barrier and backbarrier results. Numerous studies have demonstrated the importance of antecedent substrate on the morphology of modern barriers (e.g., Oertel, 1979; Belknap and Kraft, 1985), including more recent studies of U.S. East Coast barriers in which the antecedent substrate was critical to understanding the migrational history of the islands (e.g., Raff et al., 2018; Shawler et al., 2021). In this study, it was expected that lower mainland slopes would result in larger changes in shoreline position (Pilkey and Davis, 1987) and/or larger lagoon widths as mean sea level rose. However, the lagoon results in Fig. 3 show only modest index values for SLR rate and insignificant values for mainland slope. Although it is not entirely clear why mainland slope appears insensitive, two hypotheses for these interesting results are: 1) that the LTM17 model's assumption of instantaneous interior marsh growth with SLR increments reduced the mainland slope's impact on lagoon width, and/or 2) the simulation time scale was too short to produce a notable impact on the transgression rates. Additional modeling is suggested to explore this interesting result.

Most of the forcing parameters were found to significantly influence the model results, the exception being shoreface flux (Fig. 3), which is associated with how fast the shoreface is driven back toward its equilibrium state by wave climates during recovery periods between storm events. The insignificance of shoreface flux was somewhat surprising, given its demonstrated influence in helping barrier's sustain long-term behaviors such as periodic retreat and dynamic equilibrium (e.g. Lorenzo-Trueba and Ashton, 2014; Ciarletta et al., 2019) and its more detailed formulations in other models (e.g., Storms et al., 2002; Stive and de Vriend, 1995). The results were also surprising given the significance of toe depth, which, in reality, is related to shoreface flux. Taken together, these results suggest that the geometric constraints of the shoreface were more influential than the rates of shoreface response for short term simulations.

Although there were no instances of height drowning in Simulation Set C, the instances of height drowning from the preliminary results (Simulation Set A) help us understand the importance of overwash. Low

overwash values ($\leq$15 m^3/m/yr) were associated with all of the simulations that resulted in height drowning in the preliminary results (Supplemental material, Fig. S2.4). This highlights the criticality of overwash processes in maintaining the elevation of barrier islands with respect to SLR (e.g., Rosen, 1979; Ashton and Ortiz, 2011; Carruthers et al., 2013). Based on this understanding, a future increase in the frequency and localized intensity of coastal storms, which is expected among coastal scientists (e.g., Ciavola and Coco, 2017; Gopalakrishnan et al., 2018) and supported by observations and modeling studies (e.g., Bender et al., 2010; Seneviratne et al., 2023), would naturally lead to increases in overwash flux that would enable barriers to maintain their elevations. However, storm-driven overwash can also have destructive effects on barrier island morphology including beach and dune erosion, channelization of antecedent low spots, and washout (Morton and Sallenger, 2003) that are largely dependent on the storm regime (Sallenger, 2000; Stockdon et al., 2007; Plant and Stockdon, 2012). Higher storm-driven water levels generally increase in the morphological impact on barriers (Plant et al., 2017), although not in every case (Long et al., 2014). Based on modeling results from Passeri et al. (2020), increases in storminess can result in barriers changing from a narrowing (i.e., decreasing width) to a flattening (decreasing height) state and can increase the likelihood of breaching and drowning when coupled with increases in SLR. Mariotti (2021) found that sediment supply played a key role in whether or not barriers gained or lost elevation due to storms, with high sediment supply leading to accretion and low sediment supply leading to barrier flattening. The results of this study also strongly imply that where overwash is artificially reduced, height drowning is possible by the end of the century for low-relief barriers under high rates of SLR. This finding is underscored by other studies which have found anthropogenic impacts to significantly impact overwash and barrier morphology (e.g., Rogers et al., 2015; Miselis and Lorenzo-Trueba, 2017; Tenebruso et al., 2022).

While high overwash values help maintain barrier height, they can also impact the barrier width positively or negatively depending on other geometry parameters such as initial marsh width, toe depth, critical barrier width, and initial barrier width, the latter of which was fixed at 350 m for Simulation Set C. Higher overwash flux values can increase island width when critical width values are high (Fig. 6d), and since overwash removes sediment from the shoreface and subaerial island, greater change in the shoreline position is also observed (Fig. 6g). The increase in barrier width can be modulated by the initial marsh width, for which lower values offset the changes or lead to decreases in barrier width (Fig. 6f). This is because lower backbarrier marsh widths increase accommodation space, requiring additional washover volume to maintain the barrier width (Walters et al., 2014). Increases in barrier transgression are also regulated by increasing toe depth, which requires less retreat distance to achieve mass balance of the profile (Fig. 6i). In short, under high overwash conditions, barriers with low toe depths and low marsh widths were the least efficient at converting the change in shoreline position to the change in (back)barrier position, which led to reduced barrier widths. Deaton et al. (2017) observed this phenomenon in a study of U.S. East Coast barrier islands and estimated that 51% of the observed marsh loss was due to barrier transgression.

The rate of SLR was very influential on the model results, particularly for barrier transgression and marsh depth (Fig. 3). Higher rates of SLR created larger accommodation spaces that required liberated sediment from the seaward side of the transgressing barrier to fill. Thus, a direct relationship exists between the rate of SLR and rate of barrier transgression. This is in line with the previous sensitivity results (see Table 2) and is supportive of findings from other modeling studies such as Moore et al. (2007), who found that significant changes in SLR (based on Intergovernmental Panel on Climate Change projections) could result in a 150% increase in the transgression rate of the studied U.S. East Coast barrier and increase the possibility of drowning.

The results from this study showed that backbarrier marsh and lagoon dynamics were closely aligned with previous modeling studies. Parameters that were associated with the original MAC14 model, such as reference wind speed, tidal range, critical bed shear stress, and ocean sediment concentration, all impacted the backbarrier results in line with the original model (Mariotti and Carr, 2014), while the parameters associated with the original LTA14 model impacted the backbarrier results very little - the exceptions being critical barrier width and mainland slope (Fig. 3). SLR rate was a parameter in both original models (LTA14 and MAC14) and was found to be very influential across the board. Backbarrier parameters also influenced the barrier results, specifically the change in barrier width and change in shoreline position. This influence was manifested via reductions in backbarrier marsh width and depth, which increased backbarrier accommodation space and led to increased overwash volumes, decreases in barrier width, and drowning, similar to Lorenzo-Trueba and Mariotti (2017).

Critical bed shear stress, which affects the erodability of the lagoon sediment, was found to have significantly influenced the model results. Shear stress was significant both in the original simulations (Simulation Set A) where values greater than 0.2 Pa led to lagoon filling and values lower led to barrier drowning (Fig. 2c), and in the modified simulations where higher values (0.15–2.0 Pa) still led to lagoon filling and lower values (less than 0.08 Pa) were associated with width drowning (Fig. 4e). Increasing the critical bed shear stress simulates an increase in the lagoon's erosion resistance. As less lagoonal sediment is eroded, less is exported to the marsh or ocean which causes the lagoon to fill; oppositely, when critical bed shear stress is reduced, the lagoon deepens which increases marsh erosion, accommodation space, and leads to width drowning. Reeves et al. (2020) modeled the impact of modified critical bed shear stress by adding seagrass beds to the GEOMBEST+ model of Walters et al. (2014) and found very similar results as their seagrass beds act as source and sink terms for inorganic backbarrier sediment. However, they also found that decreases in seagrass beds, corresponding to a decrease in critical bed shear stress, allows the sediment that it had trapped to be exported to the marsh, resulting in marsh progradation (Reeves et al., 2020).

Ocean sediment concentration, which influences the amount of inorganic sediment deposition, was also found to have significantly influenced the model results, as low values corresponded to both width and marsh drowning (Fig. 4f). These findings support the conclusions from the original study by Lorenzo-Trueba and Mariotti (2017), who found that reduced sediment concentrations led to increased width drowning and decreased migration (see Table 2). Low ocean sediment concentrations reduce all inorganic sediment deposition in the backbarrier, thereby increasing accommodation space through reductions in marsh width, marsh depth, and lagoon depth. These results highlight the importance of considering the inorganic sediment transport dynamics in the marsh and lagoon (Fagherazzi et al., 2013; Mariotti and Fagherazzi, 2013) and suggest that tidal inlet dynamics, including the formation of new inlets (i.e., breaching), are critical morphodynamic components of the barrier island system and should be considered in long-term barrier island modeling approaches (e.g., Nienhuis and Lorenzo-Trueba, 2019; Nienhuis et al., 2021). Considering the influence of these parameters alongside the relative insignificance of overwash for the backbarrier system, these results suggest that inorganic sediment deposition through tidal inlet dispersion is much more significant to the backbarrier marsh and lagoon system than overwash over sub-centennial timescales.

6. Conclusions

The aim of the study was to gain additional insights into multi-decadal barrier-backbarrier system dynamics by exploring the parameter space of the LTM17 model using global sensitivity analysis, specifically the Sobol Method. The influence of each input parameter on the wide range of model results was tested both individually and interactively, and specific regions of sensitivity within the parameter space were identified through heatmaps of parameter interactions and boxplots of parameter values associated with distinctive simulation

categories.

Initial and critical barrier geometry parameters were found to significantly influence barrier width, height, and shoreline position through the end of this century, with narrow, low-relief barriers being most vulnerable to drowning. Width drowning was also found to be associated with multiple parameter value ranges, suggesting the risk of sub-centennial width drowning may be averted (or delayed) with a single input parameter change. The barrier profile's toe depth and the shoreface equilibrium slope, which are influenced by average wave climate, were also found to moderately influence barrier width and transgression due to conservation of mass within the barrier profile. The significant influence of critical bed shear stress and ocean sediment concentration on the backbarrier results, especially in contrast to the insignificance of overwash, suggests that inorganic sediment deposition through tidal inlet dispersion is much more significant to the backbarrier marsh and lagoon system than overwash over sub-centennial timescales.

The application of global sensitivity analysis to the LTM17 barrier island morphodynamic model using both the Sobol Method and simple factor mapping techniques has provided new insights into the modeled system dynamics and has confirmed various elements of our current understanding of barrier evolution. Future modeling studies of barrier evolution should use these sensitivity results to constrain the parameters identified as most significant and to minimize uncertainty.

CRediT authorship contribution statement

Steven W.H. Hoagland: Conceptualization, Formal analysis, Investigation, Methodology, Writing – original draft, Funding acquisition. **Jennifer L. Irish:** Conceptualization, Formal analysis, Funding acquisition, Supervision, Writing – review & editing. **Robert Weiss:** Conceptualization, Formal analysis, Funding acquisition, Supervision, Writing – review & editing.

Declaration of competing interest

The authors declare that they have no known competing financial interests or personal relationships that could have appeared to influence the work reported in this paper.

Data availability

Data will be made available on request.

Acknowledgements

This material is based upon work that is partially supported by the U. S. Army Corps of Engineers through the U.S. Coastal Research Program (under Grant No. W912HZ-20-2-0005), the National Science Foundation (under Grant Numbers 1735139 and 1630099), and Virginia Sea Grant College Program Project R/72155T funded by the National Oceanic and Atmospheric Administration's National Sea Grant College Program, U.S. Department of Commerce (under award NA18OAR4170083). The statements, findings, conclusions, and recommendations are those of the author(s) and do not necessarily reflect the views of the U.S. Army Corps of Engineers, the U.S. Coastal Research Program, the National Science Foundation, Virginia Sea Grant, the National Oceanic and Atmospheric Administration, or the U.S. Department of Commerce. The authors acknowledge Advanced Research Computing at Virginia Tech for providing computational resources and technical support that have contributed to the results reported within this paper. URL: https://arc.vt.edu/.

Appendix A. Supplementary data

Supplementary data to this article can be found online at https://doi.org/10.1016/j.geomorph.2024.109087.

References

Antolínez, J.A., Méndez, F.J., Anderson, D., Ruggiero, P., Kaminsky, G.M., 2019. Predicting climate-driven coastlines with a simple and efficient multiscale model. J. Geophys. Res. Earth 124, 1596–1624. https://doi.org/10.1029/2018JF004790.

Ashton, A.D., Lorenzo-Trueba, J., 2015. Complex responses of barriers to sea-level rise emerging from a model of alongshore-coupled dynamic profile evolution. In: The Proceedings of the Coastal Sediments 2015. World Scientific, pp. 1–7. https://doi.org/10.1142/9789814689977_0003.

Ashton, A.D., Lorenzo-Trueba, J., 2018. Morphodynamics of barrier response to sea-level rise. In: Moore, L.J., Murray, B.A. (Eds.), Barrier Dynamics and Response to Changing Climate. Springer International Publishing, pp. 277–304.

Ashton, A.D., Murray, A.B., 2006. High-angle wave instability and emergent shoreline shapes: 1. Modeling of sand waves, flying spits, and capes. J. Geophys. Res. Earth 111, 1–19. doi:https://doi.org/10.1029/2005JF000422.

Ashton, A.D., Ortiz, A.C., 2011. Overwash controls coastal barrier response to sea-level rise. In: The Proceedings of the Coastal Sediments 2011. World Scientific Publishing Company, pp. 230–243. https://doi.org/10.1142/9789814355537_0018.

Bakker, W., 1968. The dynamics of a coast with a groyne system. In: Proc. 11th ICCE. American Society of Civil Engineers, Reston, VA, pp. 492–517. https://doi.org/10.31826/9781463212209-031.

Barbier, E., Hacker, S., Kennedy, C., Koch, E., Stier, A., Silliman, B., 2011. The value of estuarine and coastal ecosystem services. Ecol. Monogr. 81 (2), 169–193.

Belknap, D.F., Kraft, J.C., 1985. Influence of antecedent geology on stratigraphic preservation potential and evolution of Delaware's barrier systems. Mar. Geol. 63, 235–262. https://doi.org/10.1016/0025-3227(85)90085-4.

Bender, M.A., Knutson, T.R., Tuleya, R.E., Sirutis, J.J., Vecchi, G.A., Garner, S.T., Held, I. M., 2010. Modeled impact of anthropogenic warming on the frequency of intense Atlantic hurricanes. Science 327, 454–458. https://doi.org/10.1126/science.1180568.

Brenner, O.T., Moore, L.J., Murray, A.B., 2015. The complex influences of back-barrier deposition, substrate slope and underlying stratigraphy in barrier island response to sea-level rise: insights from the Virginia Barrier Islands, Mid-Atlantic Bight, U.S.A. Geomorphology 246, 334–350. https://doi.org/10.1016/j.geomorph.2015.06.014.

Bridges, T.S., Wagner, P.W., Burks-copes, K.A., Bates, M.E., Collier, Z.A., Fischenich, C.J., Gailani, J.Z., Leuck, L.D., Piercy, C.D., Rosati, J.D., Russo, E.J., Shafer, D.J., Suedel, B.C., Vuxton, E.A., Wamsley, T.V., 2015. Use of Natural and Nature-based Features (NNBF) for Coastal Resilience. US Army Corps of Engineers - Engineer Research and Development Center, pp. 1–447.

Bruun, P., 1962. Sea level rise as a cause of shore erosion. Proc. ASCE Journal Waterways Harbors Div. 88, 117–130.

Buijsman, M.C., 1997. The Impact of Gas Extraction and Sea Level Rise on the Morphology of the Wadden Sea: Extension and Application of the Model ASMITA. Technical Report, Netherlands Center for Coastal Research.

Carruthers, E.A., Lane, D.P., Evans, R.L., Donnelly, J.P., Ashton, A.D., 2013. Quantifying overwash flux in barrier systems: an example from Martha's Vineyard, Massachusetts, USA. Mar. Geol. 343, 15–28. https://doi.org/10.1016/j.margeo.2013.05.013.

Ciarletta, D.J., Lorenzo-Trueba, J., Ashton, A.D., 2019. Interaction of sea-level pulses with periodically retreating barrier islands. Front. Earth Sci. 7, 1–14. https://doi.org/10.3389/feart.2019.00279.

Ciavola, P., Coco, G. (Eds.), 2017. Coastal Storms. John Wiley & Sons, Ltd, Chichester, UK. doi:https://doi.org/10.1002/9781118937099.

Cowell, P.J., Kinsela, M.A., 2018. Shoreface controls on barrier evolution and shoreline change. In: Moore, L.J., Murray, B.A. (Eds.), Barrier Dynamics and Response to Changing Climate. Springer International Publishing, pp. 243–275.

Cowell, P., Roy, P., Jones, R., 1992. Shoreface translation model: computer simulation of coastal-sandbody response to sea level rise. Math. Comput. Simul. 33, 603–608.

Cowell, P., Roy, P.S., Jones, R.A., 1995. Simulation of large-scale coastal change using a morphological behaviour model. Mar. Geol. 126, 45–61. https://doi.org/10.1016/0025-3227(95)00065-7.

Cowell, P.J., Stive, M.J., Niedoroda, A.W., Swift, D.J., De Vriend, H.J., Buijsman, M.C., Nicholls, R.J., Roy, P.S., Kaminsky, G.M., Cleveringa, J., Reed, C.W., De Boer, P.L., 2003. The coastal-tract (part 2): applications of aggregated modeling of lower-order coastal change. J. Coast. Res. 19, 828–848.

Dean, R.G., Houston, J.R., 2016. Determining shoreline response to sea level rise. Coast. Eng. 114, 1–8. https://doi.org/10.1016/j.coastaleng.2016.03.009.

Dean, R.G., Maurmeyer, E., 1983. Models for beach profile response. In: Komar, P.D. (Ed.), Handbook of Coastal Processes and Erosion. CRC Press, Taylor and Francis Group, pp. 151–166 (chapter 7).

Deaton, C.D., Hein, C.J., Kirwan, M.L., 2017. Barrier island migration dominates ecogeomorphic feedbacks and drives salt marsh loss along the Virginia Atlantic Coast, USA. Geology 45, 123–126. https://doi.org/10.1130/G38459.1.

Everts, C.H., 1985. Sea level rise effects on shoreline position. J. Waterw. Port Coast. Ocean Eng. 111, 985–999.

Everts, C.H., 1987. Continental shelf evolution in response to a rise in sea level. In: Sea-level Fluctuations and Coastal Evolution. SEPM. Society for Sedimentary Geology, pp. 49–57. https://doi.org/10.2110/pec.87.41.0049. URL: https://pubs.geoscienceworld.org/books/book/1045/chapter/10534595/.

Fagherazzi, S., Mariotti, G., Wiberg, P.L., 2013. Marsh collapse does not require sea level rise. Oceanography 26, 70–77. https://doi.org/10.5670/oceanog.2013.47.

Frey, A.E., Connell, K.J., Hanson, H., Larson, M., Thomas, R.C., Munger, S., Zundel, A., 2012. GenCade Version 1 Model Theory and User's Guide. Technical Report December, US Army Corps of Engineers, Coastal and Hydraulics Laboratory.

Gopalakrishnan, S., Landry, C.E., Smith, M.D., 2018. Climate change adaptation in coastal environments: modeling challenges for resource and environmental

economists. Rev. Environ. Econ. Policy 12, 48–68. https://doi.org/10.1093/reep/rex020.
Grzegorzewski, A.S., Cialone, M.A., Wamsley, T.V., 2011. Interaction of barrier islands and storms: implications for flood risk reduction in Louisiana and Mississippi. J. Coast. Res. 59, 156–164. https://doi.org/10.2112/si59-016.1.
Hallermeier, R.J., 1977. Calculating a Yearly Limit Depth to the Active Beach Profile. Technical Report. U.S, Army Corps of Engineers, Coastal Engineering Research Center.
Hallermeier, R.J., 1980. A profile zonation for seasonal sand beaches from wave climate. Coast. Eng. 4, 253–277. https://doi.org/10.1016/0378-3839(80)90022-8.
Hanson, H., 1989. GENESIS - a generalized shoreline change numerical model. J. Coast. Res. 5, 1–27.
Hoagland, S.W., Jeffries, C.R., Irish, J.L., Weiss, R., Mandli, K., Vitousek, S., Johnson, C. M., Cialone, M.A., 2023. Advances in morphodynamic modeling of coastal barriers: a review. J. Waterw. Port Coast. Ocean Eng. 149 https://doi.org/10.1061/JWPED5.WWENG-1825.
Larson, M., Kraus, N.C., Hanson, H., 1990. Decoupled numerical model of three-dimensional beach change. In: Proc. 22nd ICCE. American Society of Civil Engineers, Delft, The Netherlands, pp. 2173–2185.
Larson, M., Kraus, N.C., Hanson, H., 2002. Simulation of regional longshore sediment transport and coastal evolution - the "cascade" model. In: Coastal Engineering 2002. World Scientific Publishing Company, pp. 2612–2624. https://doi.org/10.1142/9789812791306_0218.
Leatherman, S.P., 1979. Migration of Assateague Island, Maryland, by inlet and overwash processes. Geology 7, 104–107.
Long, J.W., de Bakker, A.T., Plant, N.G., 2014. Scaling coastal dune elevation changes across storm-impact regimes. Geophys. Res. Lett. 41, 2899–2906. https://doi.org/10.1002/2014GL059616.
Lorenzo-Trueba, J., Ashton, A.D., 2014. Rollover, drowning, and discontinuous retreat: distrinct modes of barrier response to sea-level rise arising from a simple morphodynamic model. J. Geophys. Res. Earth 779–801. https://doi.org/10.1002/2013JF002871.Received.
Lorenzo-Trueba, J., Mariotti, G., 2017. Chasing boundaries and cascade effects in a coupled barrier-marshlagoon system. Geomorphology 290, 153–163. https://doi.org/10.1016/j.geomorph.2017.04.019.
Mariotti, G., 2021. Self-organization of coastal barrier systems during the Holocene. J. Geophys. Res. Earth 126, 1–23. https://doi.org/10.1029/2020JF005867.
Mariotti, G., Carr, J., 2014. Dual role of salt marsh retreat: long-term and short-term resilience. Water Resour. Res. 50, 2963–2974. https://doi.org/10.1002/2013WR014676.
Mariotti, G., Fagherazzi, S., 2013. Critical width of tidal flats triggers marsh collapse in the absence of sea-level rise. Proc. Natl. Acad. Sci. U. S. A. 110, 5353–5356. https://doi.org/10.1073/pnas.1219600110.
McBride, R.A., Anderson, J.B., Buynevich, I.V., Byrnes, M.R., Cleary, W., Fenster, M.S., FitzGerald, D.M., Hapke, C.J., Harris, M.S., Hein, C.J., Johnson, C.L., Klein, A.H., Liu, B., De Menezes, J.T., Mulhern, J.S., Oliver, T.S., Pejrup, M., Riggs, S.R., Roberts, H.H., Rodriguez, A.B., Seminack, C.T., Short, A.D., Stone, G.W., Tamura, T., Wallace, D.J., Wang, P., 2022. Morphodynamics of Modern and Ancient Barrier Systems: An Updated and Expanded Synthesis, , second ed.vol. 8. Elsevier. https://doi.org/10.1016/B978-0-12-818234-5.00153-X.
McCarroll, R.J., Masselink, G., Valiente, N.G., Scott, T., Wiggins, M., Kirby, J.A., Davidson, M.A., 2021. A rules-based shoreface translation and sediment budgeting tool for estimating coastal change: ShoreTrans. Mar. Geol. 435, 106466 https://doi.org/10.1016/j.margeo.2021.106466.
Miselis, J.L., Lorenzo-Trueba, J., 2017. Natural and human-induced variability in barrier-island response to sea level rise. Geophys. Res. Lett. 44, 911–922. https://doi.org/10.1002/2017GL074811.
Moore, L.J., Murray, A.B. (Eds.), 2018. Barrier Dynamics and Response to Changing Climate. Springer International Publishing, Cham, Switzerland. https://doi.org/10.1007/978-3-319-68086-6.
Moore, L.J., List, J.H., Williams, S.J., Stolper, D., 2007. Modeling barrier island response to sea-level rise in the outer banks, North Carolina. In: Coastal Sediments '07. American Society of Civil Engineers, Reston, VA, pp. 1153–1164.
Moore, L.J., List, J.H., Williams, S.J., Stolper, D., 2010. Complexities in barrier island response to sea level rise: insights from numerical model experiments, North Carolina Outer Banks. J. Geophys. Res. 115, F03004 https://doi.org/10.1029/2009jf001299.
Morton, R.A., Sallenger, A.H., 2003. Morphological impacts of extreme storms on sandy beaches and barriers. J. Coast. Res. 19, 560–573.
Murray, B.A., Moore, L.J., 2018. Geometric constraints on long-term barrier migration: from simple to surprising. In: Moore, L.J., Murray, B.A. (Eds.), Barrier Dynamics and Response to Changing Climate. Springer International Publishing, pp. 211–242.
Nicholls, R.J., Birkemeier, W.A., Lee, G.h., 1998. Evaluation of depth of closure using data from Duck, NC, USA. Mar. Geol. 148, 179–201. https://doi.org/10.1111/j.1365-2427.2008.02031.x.
Niedoroda, A.W., Reed, C.W., Swift, D.J., Arato, H., Hoyanagi, K., 1995. Modeling shore-normal large-scale coastal evolution. Mar. Geol. 126, 181–199. URL: doi:https://doi.org/10.1016/0025-3227(95)98961-7.
Nienhuis, J.H., Lorenzo-Trueba, J., 2019. Simulating barrier island response to sea level rise with the barrier island and inlet environment (BRIE) model v1.0. Geosci. Model Dev. 12, 4013–4030. https://doi.org/10.5194/gmd-12-4013-2019.
Nienhuis, J.H., Heijkers, L.G., Ruessink, G., 2021. Barrier breaching versus overwash deposition: predicting the morphologic impact of storms on coastal barriers. J. Geophys. Res. Earth 126, 1–17. https://doi.org/10.1029/2021JF006066.
Oertel, G.F., 1979. Barrier island development during the Holocene recession, southeastern United States. In: Leatherman, S.P. (Ed.), Barrier Islands: From the Gulf of St. Lawrence to the Gulf of Mexico. Academic Press, pp. 273–290.
Ortiz, A.C., Ashton, A.D., 2016. Exploring shoreface dynamics and a mechanistic explanation for a morphodynamic depth of closure, Journal of Geophysical Research: Earth Surface. https://doi.org/10.1002/2013JF002871.
Palalane, J., Larson, M., 2020. A long-term coastal evolution model with longshore and cross-shore transport. J. Coast. Res. 36, 411–423. https://doi.org/10.2112/JCOASTRES-D-17-00020.1.
Passeri, D.L., Dalyander, P.S., Long, J.W., Mickey, R.C., Jenkins, R.L., Thompson, D.M., Plant, N.G., Godsey, E.S., Gonzalez, V.M., 2020. The roles of storminess and sea level rise in decadal barrier island evolution. Geophys. Res. Lett. 47, 1–8. https://doi.org/10.1029/2020GL089370.
Pelnard-Considere, R., 1956. Essai de theorie de l'evolution des formes de rivage en plages de sable et de galets. Journees de L'hydraulique 289–298.
Perlin, M., Dean, R.G., 1979. Prediction of beach planforms with littoral controls. Proc. Coast. Eng. Conf. 2, 1818–1838. https://doi.org/10.9753/icce.v16.110.
Pilkey, O.H., Davis, T.W., 1987. An analysis of coastal recession models: North Carolina coast. In: Sea-level Fluctuation and Coastal Evolution. SEPM (Society for Sedimentary Geology), pp. 59–68.
Plant, N.G., Stockdon, H.F., 2012. Probabilistic prediction of barrier-island response to hurricanes. J. Geophys. Res. Earth 117, 1–17. https://doi.org/10.1029/2011JF002326.
Plant, N., Doran, K., Stockdon, H., 2017. Examples of storm impacts on barrier islands. In: Coastal Storms. Wiley, pp. 65–79. https://doi.org/10.1002/9781118937099.ch4.
Raff, J.L., Shawler, J.L., Ciarletta, D.J., Hein, E.A., Lorenzo-Trueba, J., Hein, C.J., 2018. Insights into barrier-island stability derived from transgressive/regressive state changes of Parramore Island, Virginia. Mar. Geol. 403, 1–19. https://doi.org/10.1016/j.margeo.2018.04.007.
Razavi, S., Gupta, H.V., 2016. A new framework for comprehensive, robust, and efficient global sensitivity analysis: 1. Theory. Water Resour. Res. 52, 423–439. https://doi.org/10.1002/2015WR017558.
Reeves, I.R., Moore, L.J., Goldstein, E.B., Murray, A.B., Carr, J.A., Kirwan, M.L., 2020. Impacts of seagrass dynamics on the coupled long-term evolution of barrier-marsh-bay systems. J. Geophys. Res. Biogeosci. 125, 1–19. https://doi.org/10.1029/2019JG005416.
Reeves, I.R., Moore, L.J., Murray, A.B., Anarde, K.A., Goldstein, E.B., 2021. Dune dynamics drive discontinuous barrier retreat. Geophys. Res. Lett. 48, 1–11. https://doi.org/10.1029/2021GL092958.
Robbins, M.G., Shawler, J.L., Hein, C.J., 2022. Contribution of longshore sand exchanges to mesoscale barrier-island behavior: insights from the Virginia Barrier Islands, U.S. East Coast. Geomorphology 403, 108163. https://doi.org/10.1016/j.geomorph.2022.108163.
Rogers, L.J., Moore, L.J., Goldstein, E.B., Hein, C.J., Lorenzo-trueba, J., Ashton, A.D., 2015. Anthropogenic controls on overwash deposition: evidence and consequences. J. Geophys. Res. Earth 2609–2624. https://doi.org/10.1002/2015JF003634.
Rosati, J.D., Dean, R.G., Kraus, N.C., Stone, G.W., 2006. Morphologic evolution of subsiding barrier island systems. In: Coastal Engineering 2006. World Scientific Publishing Company, San Diego, California, pp. 3963–3975. https://doi.org/10.1142/9789812709554_0333.
Rosati, J.D., Dean, R.G., Stone, G.W., 2010. A cross-shore model of barrier island migration over a compressible substrate. Mar. Geol. 271, 1–16. https://doi.org/10.1016/j.margeo.2010.01.005.
Rosati, J.D., Dean, R.G., Walton, T.L., 2013. The modified Bruun Rule extended for landward transport. Mar. Geol. 340, 71–81. https://doi.org/10.1016/j.margeo.2013.04.018.
Rosen, P.S., 1979. Aeolian dynamics of a barrier island system. In: Leatherman, S.P. (Ed.), Barrier Islands: From the Gulf of St. Lawrence to the Gulf of Mexico. Academic Press, pp. 81–98.
Sallenger, A.H., 2000. Storm impact scale for barrier islands. J. Coast. Res. 16, 890–895.
Saltelli, A., Ratto, M., Andres, T., Campolongo, F., Cariboni, J., Gatelli, D., Saisana, M., Tarantola, S., 2008. Global Sensitivity Analysis. The Primer. Wiley, Chichester, UK. https://doi.org/10.1002/9780470725184.
Seneviratne, S., Zhang, X., Adnan, M., Badi, W., Dereczynski, C., Luca, A.D., Ghosh, S., Iskandar, I., Kossin, J., Lewis, S., Otto, F., Pinto, I., Satoh, M., Vicente-Serrano, S., Wehner, M., Zhou, B., 2023. Weather and climate extreme events in a changing climate. In: Climate Change 2021 – The Physical Science Basis. Cambridge University Press, pp. 1513–1766. https://doi.org/10.1017/9781009157896.013. URL: https://www.cambridge.org/core/product/identifier/9781009157896%23c11/type/book_part.
Shawler, J.L., Ciarletta, D.J., Connell, J.E., Boggs, B.Q., Lorenzo-Trueba, J., Hein, C.J., 2021. Relative influence of antecedent topography and sea-level rise on barrier-island migration. Sedimentology 68, 639–669. https://doi.org/10.1111/sed.12798.
Sobol, I., 1993. Sensitivity estimates for nonlinear mathematical models. Mathematical Modelling and Computational Experiment 1, 407–414.
Stive, M.J., de Vriend, H.J., 1995. Modelling shoreface profile evolution. Mar. Geol. 126, 235–248. URL: doi:https://doi.org/10.1016/0025-3227(95)00080-I.
Stockdon, H.F., Sallenger, A.H., Holman, R.A., Howd, P.A., 2007. A simple model for the spatially-variable coastal response to hurricanes. Mar. Geol. 238, 1–20. https://doi.org/10.1016/j.margeo.2006.11.004.
Stolper, D., List, J.H., Thieler, E.R., 2005. Simulating the evolution of coastal morphology and stratigraphy with a new morphological-behaviour model (GEOMBEST). Mar. Geol. 218, 17–36. https://doi.org/10.1016/j.margeo.2005.02.019.
Storms, J.E., Weltje, G., van Dijke, J., Geel, C., Kroonenberg, S., 2002. Process-response modeling of wave-dominated coastal systems: simulating evolution and stratigraphy

on geological timescales. J. Sediment. Res. 72, 226–239. https://doi.org/10.1306/052501720226.

Stutz, M.L., Pilkey, O.H., 2011. Open-ocean barrier islands: global influence of climatic, oceanographic, and depositional settings. J. Coast. Res. 272, 207–222. https://doi.org/10.2112/09-1190.1.

Swart, D.H., 1974. Offshore Sediment Transport and Equilibrium Beach Profiles. Bibliotheek Technische Universiteit (Ph.D. thesis).

Tenebruso, C., Nichols-O'Neill, S., Lorenzo-Trueba, J., Ciarletta, D.J., Miselis, J.L., 2022. Undeveloped and developed phases in the centennial evolution of a barrier-marsh-lagoon system: the case of Long Beach Island, New Jersey. Front. Mar. Sci. 9, 1–15. https://doi.org/10.3389/fmars.2022.958573.

VGIN, 2021. Virginia Base Mapping Program (VBMP) Orthoimagery. URL. https://vgin.vdem.virginia.gov/pages/base-mapping.

de Vriend, H.J., Capobianco, M., Chesher, T., de Swart, H.E., Latteux, B., Stive, M.J., 1993. Approaches to long-term modelling of coastal morphology: a review. Coast. Eng. 21, 225–269. https://doi.org/10.1016/0378-3839(93)90051-9.

Walters, D., Moore, L.J., Vinent, O.D., Fagherazzi, S., Mariotti, G., 2014. Interactions between barrier islands and backbarrier marshes affect island system response to sea level rise: insights from a coupled model. J. Geophys. Res. Earth 2013–2031. https://doi.org/10.1002/2014JF003091.

Wolinsky, M.A., Murray, A.B., 2009. A unifying framework for shoreline migration: 2. Application to wave-dominated coasts. J. Geophys. Res. Earth 114, 1–13. https://doi.org/10.1029/2007JF000856.